MLSO Mark III K-Coronameter *Observations of the CME Rate from 1989–1996*

O. C. St. Cyr, Q. A. Flint, H. Xie, D. F. Webb, J. T. Burkepile, A. R. Lecinski, C. Quirk & A. L. Stanger

Solar Physics
A Journal for Solar and Solar-Stellar Research and the Study of Solar Terrestrial Physics

ISSN 0038-0938

Sol Phys
DOI 10.1007/s11207-015-0780-2

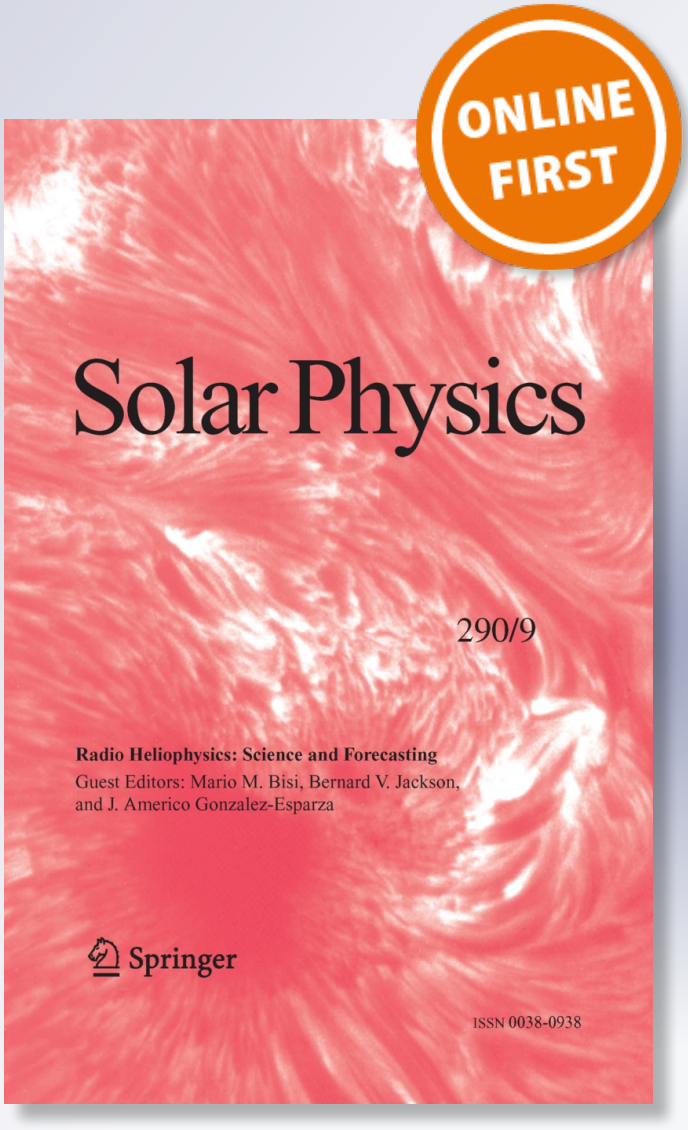

Springer

Solar Phys
DOI 10.1007/s11207-015-0780-2

MLSO *Mark III K-Coronameter* Observations of the CME Rate from 1989 – 1996

O.C. St. Cyr[1,2] · Q.A. Flint[2,3] · H. Xie[2] · D.F. Webb[4] · J.T. Burkepile[5] · A.R. Lecinski[5] · C. Quirk[2] · A.L. Stanger[5]

Received: 6 March 2015 / Accepted: 14 September 2015

Abstract We report here an attempt to fill the 1990 – 1995 gap in the CME rate using the Mauna Loa Solar Observatory's *Mark III* (Mk3) *K-coronameter*. The Mk3 instrument observed routinely several hours most days beginning in 1980 until it was upgraded to Mk4 in 1999. We describe the statistical properties of the CMEs detected during 1989 – 1996, and we determine a CME rate for each of those years. Since spaceborne coronagraphs have more complete duty cycles than a ground-based instrument at a single location, we compare the Mk3-derived CME rate from 1989 with the rate from the SMM C/P coronagraph, and from 1996 with the rate from the SOHO LASCO coronagraphs.

Keywords Solar corona · Coronal mass ejections · Solar activity

1. Introduction

Coronagraphs observe the extended atmosphere of our star, the Sun. Since their invention in the 1930s (Lyot, 1933) they have provided useful measurements for a wide variety of scientific topics (*e.g.*, St. Cyr, Fleck, and Davila, 2014). In the mid-1950s, a ground-based coronagraph was deployed at the Climax Observatory (Wlerick and Axtell, 1957) to provide routine observations of the electron-scattered (*aka* "white-light" or "K") corona. This instrument (later called "*Mark I*") produced photometric measurements by scanning at a variety of altitudes above the photosphere and, although it did not produce images, it was nevertheless useful for research (*e.g.*, Newkirk, Axtell, and Wlerick, 1957; Newkirk *et al.*, 1959). The instrument was moved from Colorado to Mees Solar Observatory

✉ O.C. St. Cyr
chris.stcyr@nasa.gov

1 Code 670, NASA-GSFC, Greenbelt, MD 20771, USA

2 Department of Physics, The Catholic University of America, Washington, DC 20064, USA

3 Gustavus Adolphus College, St. Peter, MN 56082, USA

4 Institute for Scientific Research, Boston College, Chestnut Hill, MA 02467, USA

5 High Altitude Observatory, Boulder, CO 80301, USA

Published online: 27 October 2015

on Haleakala in late 1963; and it was subsequently redeployed to Mauna Loa Solar Observatory (MLSO) in 1965 (Hansen, Garcia, and Hansen, 1969). Additional improvements to the instrument (*Mark II*) were reported by Garcia *et al.* (1971), and ground-based imaging of the white-light corona was finally realized with the *Mark III K-coronameter* (hereafter referred to as Mk3) in 1980 (Fisher *et al.*, 1981).

The Mk3 used novel internal-occultation techniques to image the lower corona (from 1.12–2.44 R_{Sun}), and it was deployed in time to complement the middle corona field of view ($\sim$2–5 R_{Sun}) of the externally occulted coronagraph/polarimeter on NASA's *Solar Maximum Mission* (SMM C/P; MacQueen *et al.*, 1980). The Mk3 operated more-or-less continuously through the 1980s and 1990s until it was upgraded to Mk4 in September 1999 (Elmore *et al.*, 2003). Recently the Mk4 was retired and replaced in late 2013 with K-Cor (De Wijn *et al.*, 2012), which permits measurements even closer to the solar disk (1.05–3.0 R_{Sun}) with significant improvements in spatial resolution and temporal cadence.

Observing at MLSO is, of course, limited by the day-night cycle and by sky conditions, with the best seeing typically occurring in the hours immediately following local sunrise. The MLSO coronagraphic observations have been widely used to study the formation and initial dynamics of coronal mass ejections (CMEs) as well as other scientific topics, and we refer the interested reader to the online publication listing (http://www2.hao.ucar.edu/mlso/mlso-publications).

Measurements of the properties of CMEs in the low corona are important for several reasons. Foremost, CMEs accelerate most rapidly in the low corona, which is below the field of view of externally occulted spaceborne coronagraphs. CME trajectories measured by spaceborne coronagraphs can usually be characterized by a single (constant) speed: *e.g.*, $\sim$80 % of the speeds in the compilation of SMM CMEs (Burkepile and St. Cyr, 1993) and SOHO LASCO CMEs (St. Cyr *et al.*, 2000). So observations very low in the corona are necessary to detect the acceleration mechanisms that produce the constant speeds of CMEs through the middle corona. Similarly, measurements of the initial expansion of a CME provide constraints to models of the initiation of these eruptions.

With the availability of quasi-continuous solar observation by space-based platforms, ground-based telescopes have not been routinely used to determine the frequency or probability of sporadic solar phenomena such as CMEs. Based on numerous measurement platforms, Webb and Howard (1994) reported the CME occurrence rate over the extended time period from 1972 – 1989. The primary data sources for that analysis were space-based instruments (*Skylab*, *Helios*, *Solwind*, and SMM). Since the launch of SOHO in late 1995 (*e.g.*, Domingo, Fleck, and Poland, 1995) the LASCO coronagraphs (Brueckner *et al.*, 1995) have provided a nearly continuous measure of CME activity to the present date. Therefore the only remaining gap in the CME record since the early 1970s has been the period from late-1989 to early-1996.

To fill this gap in the historic CME rate, we have examined MLSO Mk3 observations and report those results here. In the sections below we report on the observations and the properties of Mk3 CMEs during this gap in spaceborne observations, and we describe our method to determine a "duty cycle" to normalize the limited observations to an annual CME rate. We also discuss the comparison of the Mk3 CME rate to that derived from SMM (1989) and from LASCO (1996).

2. Observations, Measurements, Statistical Properties of CMEs with Mk3

The observations and properties of CMEs detected by Mk3 between 1980 and 1989 were described by St. Cyr *et al.* (1999, hereafter referred to as Paper1). The Mk3 telescope mea-

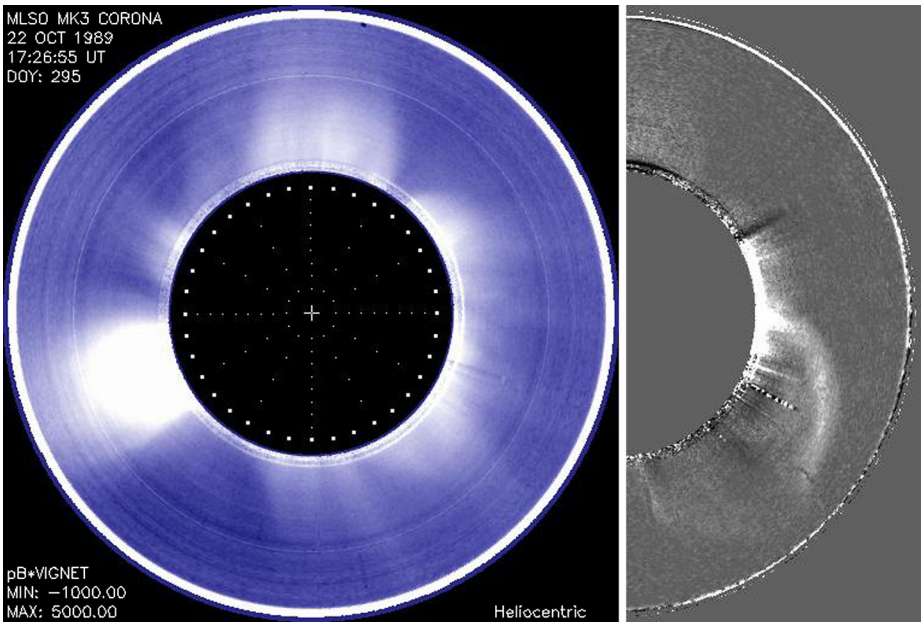

Figure 1 On the left, a MLSO Mk3 image from October 22, 1989. The size and location of the Sun are depicted by the dotted circle on the shadow of the occulting disk, and the image is oriented with solar North up. On the right, a very fast ($> 1000\ \mathrm{km\,s^{-1}}$) loop CME is seen in the SW in the single frame taken at 17:45 U.T., a difference image created by subtracting the earlier image taken at 17:26 U.T., shown on the left.

sured the polarization brightness of the photospheric radiation scattered by free electrons in the bandpass 680 – 1100 nm. The Mk3 used a linear diode array that was swept azimuthally to produce a complete scan of 360° in position angle in about three minutes. The archive of Mk3 images (formatted as FITS files) is available electronically at http://www2.hao.ucar.edu. An example of a fast CME ($1030\ \mathrm{km\,s^{-1}}$) imaged by Mk3 is shown in Figure 1. This CME was associated with a ground-level solar particle event (Shea *et al.*, 1995) but occurred during an SMM C/P data gap.

As in Paper1, CMEs were detected by examining time-ordered sequences of direct images as well as images differenced from an earlier pre-event image each day. The following information was recorded for each CME: time of first detection; apparent location (measured as central position angle and converted to apparent central latitude); apparent azimuthal size; apparent speed (where possible); estimated brightness (1 – 3); and a brief description of the morphology of the event. The electronic CME list of individual events is available online in tabular form at the MLSO website [mlso.hao.ucar.edu/cgi-bin/mlso_events_Drup.cgi]. Table 1 gives the annual statistics for the Mk3 CME observations. In our examination of the data, it was a combination of the appearance of new bright material exhibiting an outward motion that qualified as a CME. The deflection of an existing coronal feature did not in itself indicate a new CME, but it was not unusual to detect an event when significant deflections were seen.

The location, size, and speed distributions of CMEs, and their behavior over the solar cycle are well known (*e.g.*, Howard *et al.*, 1985; Hundhausen, 1993; Hundhausen, Burkepile, and St. Cyr, 1994; Hundhausen, Stanger, and Serbicki, 1994; St. Cyr *et al.*, 1999; St. Cyr *et al.*, 2000; Yashiro, Michalek, and Gopalswamy, 2008; Robbrecht, Berghmans,

Table 1 This table displays the overall annual statistics for MLSO Mk3 observations of CMEs. See the text for further description of the two methods for calculating equivalent observing time; calculation of the CME rate; and for the (correction) that has been applied for the discarded data due to the "synoptic-only" program in 1989.

	1989	1990	1991	1992	1993	1994	1995	1996
Days with any observation [Days]	231 (68)	206	250	231	191	248	256	233
Equivalent observing time [Days] observing time less 10^{min} data gaps	22.98 (5.92)	19.56	26.54	28.58	26.57	42.09	42.64	38.14
Equivalent observing time [Days] producing usable images	20.27 (5.97)	17.08	22.08	22.60	19.94	30.51	31.16	26.68
Number of CMEs	66	46	57	52	18	11	18	6
CME Rate [CMEs/day]	$3.1 + 0.6/-0.2$	2.5 ± 0.2	2.4 ± 0.2	2.1 ± 0.2	0.8 ± 0.1	0.3 ± 0.05	0.5 ± 0.1	0.2 ± 0.03

and van der Linden, 2009). The properties of the 1989 – 1996 Mk3 CMEs follow similar statistical distributions to these earlier references. In Figure 2a, we show the apparent central latitude distribution, which is fairly symmetric around the equator. The CMEs from this period appeared with a slight preference to the west limb (58 %); but they were equally split northern (49 %) versus southern (51 %) hemisphere. In Figure 2b, we show the asymmetric distribution of apparent widths, with the peak of the distribution is in the 21° – 30° bin. The average size (36°) is almost identical to that found in Paper1. In Figure 2c we show the asymmetric distribution of apparent speeds for the 181 events where that measurement was possible. The average speed was 399 km s^{-1} (again, almost identical to the 390 km s^{-1} average reported in Paper1); and the maximum apparent speed was 1808 km s^{-1} (October 25, 1990).

In addition to the usual parameters, we estimated the "brightness" for each CME during this study, and that distribution is shown in Figure 2d. The categories were Very Faint (1, only detected in difference images); Faint (2, detected in difference images, but then could be identified in direct images); and Bright (3, easily seen in direct images). This parameter should be useful in a planned future study comparing the historic CME rate, so we document it here. We will return to this parameter in the Discussion section.

3. Mk3 Duty Cycle Calculation and CME Rate

Space-based coronagraphs observe the solar atmosphere with a cadence designed to match the transit of the desired phenomenon across the instrumental field of view, and often the cadence can be limited by the available telemetry downlink capacity. The duty-cycle calculation for a space-based coronagraph is therefore fairly straightforward, and examples have been documented based on CME speed (Hundhausen, Burkepile, and St. Cyr, 1994); on sun-grazing comet occurrences (MacQueen and St. Cyr, 1991; and Biesecker *et al.*, 2002); and for the CME rate (Webb and Howard, 1994). Recently Wang and Colaninno (2014) have examined the impact of image cadence on the CME rate derived from LASCO observations.

The CME rates from space-based coronagraphs are typically cited in units of [CMEs/day] with an uncertainty determined by the duty cycle. Because of their quasi-continuous observations, meaningful CME rates can be determined for space-based coronagraphs on as short a time-scale as a Carrington Rotation (*e.g.*, St. Cyr *et al.*, 2000). But for a ground-based

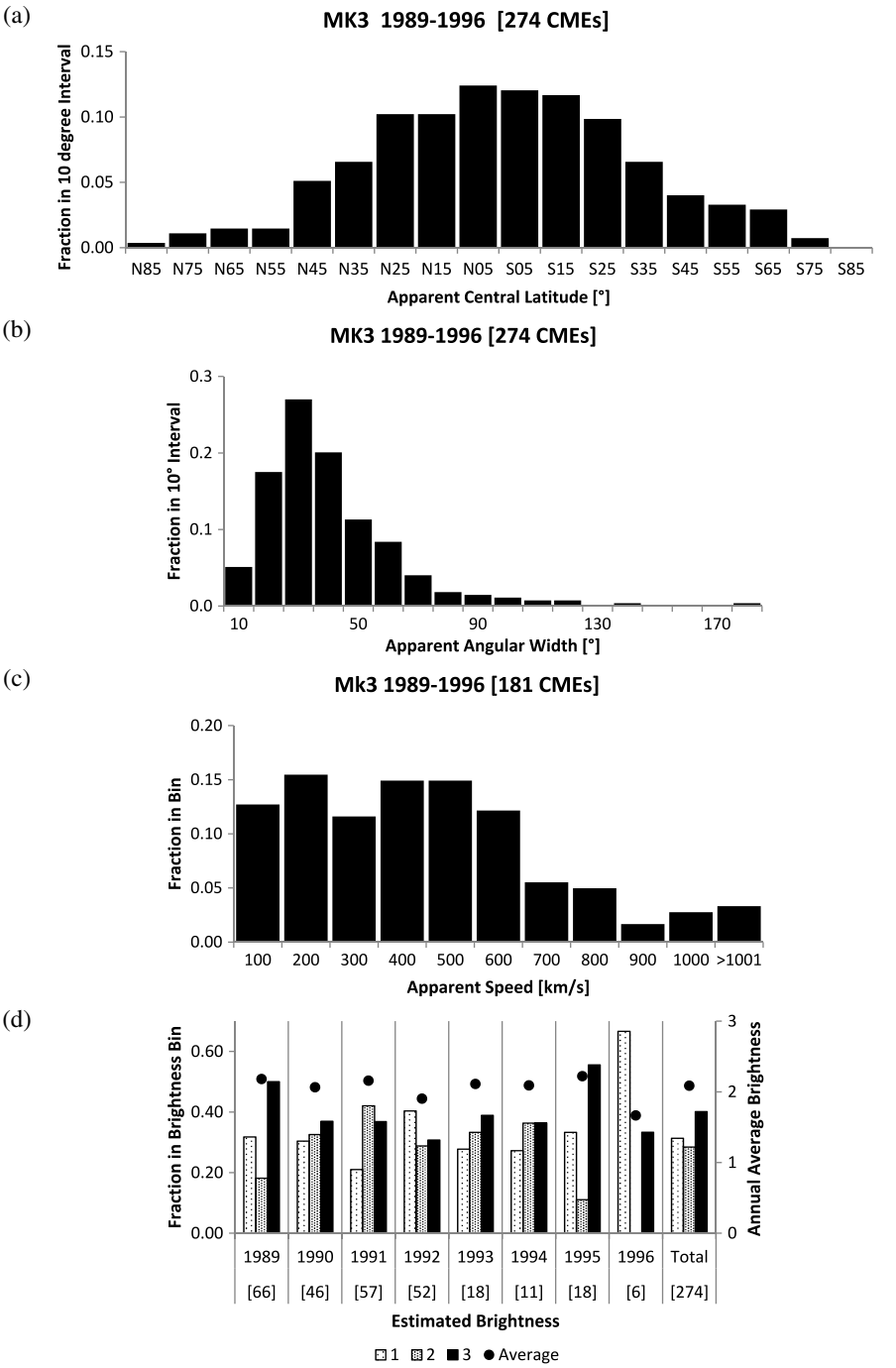

Figure 2 (a) The distribution of apparent locations for the Mk3 CMEs 1989 – 1996. (b) The distribution of apparent sizes for the Mk3 CMEs 1989 – 1996. (c) The distribution of apparent speeds for the Mk3 CMEs 1989 – 1996. (d) The distribution of estimated brightness for the Mk3 CMEs 1989 – 1996. The dots indicate the average brightness in each calendar year.

instrument in a single location that observed only a few hours each day and a limited number of days each year, the normalization for comparison to space-based coronagraphs will naturally be much larger. However, even with that limitation, we have found that annualized CME rates with realistic uncertainty estimates are achievable.

Here we describe three techniques we have employed to calculate the Mk3 observing duty cycle:

- *Observing time duration, less any data gaps*. This is more-or-less direct, and it provides a primary estimate of the amount of time the coronagraph was acquiring coronal data. But on most days there are interruptions in the three minute cadence between the time of the first image and the time of the final image due to instrumental problems or the temporary deterioration of sky conditions, so we need to compensate for these gaps. Based on the 140 Mk3 events measured between 1980 and 1989 [Paper1], about 10 % of the CMEs were faster than 800 $\mathrm{km\,s^{-1}}$, and the maximum speed measured was 1534 $\mathrm{km\,s^{-1}}$. A CME traveling 1500 $\mathrm{km\,s^{-1}}$ would be visible for about 10 minutes in the Mk3 field of view, so for a conservative estimate we have subtracted all gaps in coverage that were that length or greater. This adjusted value of observing time duration (listed as the first Equivalent Observing Time in Table 1) then provides us with our first measure of a duty cycle for Mk3.
- *Total number of images acquired, less any bad images*. Since Mk3 images were acquired every three minutes, an alternate method to determine the duty cycle is to tally the number of images acquired each day, and subtract any that were not useful for detecting CMEs. We rejected an image as "bad" if the corona was not visible or was missing over a significant portion of the image (*i.e.*, about a quarter or more of the 360 degree scan). This might have occurred because the scan was interrupted, because electronic noise appeared during the scan, or because sky conditions deteriorated during the scan. Although the latter case could occur at any time, the observing conditions at MLSO are typically best at sunrise, and sky deterioration was often the limiting case that defined the end of an observing run on a given day. The tally of "useful" images (listed as the second Equivalent Observing Time) is then a second measure of the Mk3 duty cycle.
- *"Synoptic-only" correction (1989 only)*. Following the interruption of SMM C/P observations in late 1980 (*e.g.*, Woodgate and Maran, 1986), Mk3 observations from 1981 – 1989 were routinely discarded when the observer-on-duty did not detect a CME. In Paper1 we noted a category "synoptic-only" that had been tabulated separately from days with "no observation" in the Mk3 archive. This situation arose as a result of a procedural change beginning in 1981 when only two images were retained each observing day as part of a synoptic program, and that practice ended during 1989. We will return to this topic in the Discussion section.

As one can see in Table 1, the equivalent observing time based on actual time (less 10 minute data gaps) provides an upper limit, producing a smaller CME rate when compared to the equivalent time based on the number of usable images. The latter reflects the fact that individual bad frames appear throughout an observing day, so this value underestimates the equivalent observing time and yields a larger CME rate. Similar to the 10 minute gaps, we have also tallied the duration of 19 minute and 40 minute data gaps (corresponding to 800 $\mathrm{km\,s^{-1}}$ and 400 $\mathrm{km\,s^{-1}}$ speeds), but the effect on the rate calculation was smaller than 0.1 CMEs/day. Therefore we believe that the best determination of the CME rate is the average of the two rates based on the equivalent observing time (10 minute gaps) and on the useable number of images, with the uncertainty estimate being the difference between the two. For 1989 only, we have increased the estimated uncertainties because of the "synoptic-only" days, and we address how that was done in the Discussion section.

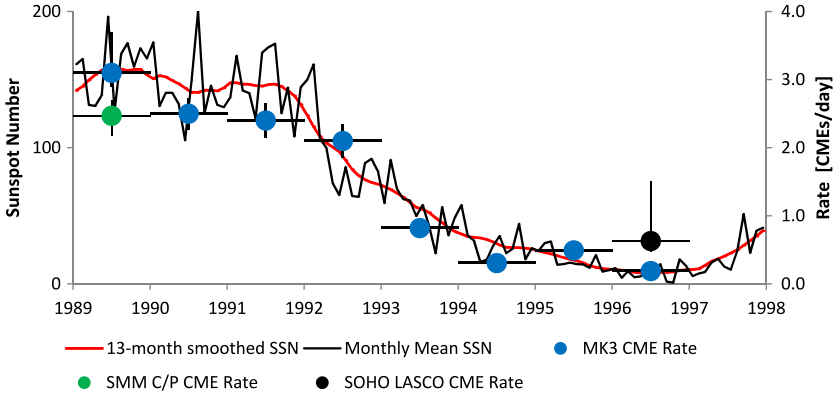

Figure 3 Scatter plot of the annual CME rate [CMEs/day] based on observations from Mk3 (1989 – 1996), SMM C/P (1989), and SOHO LASCO (1996). The monthly and 13-month-smoothed sunspot number are also shown.

The Mk3 CME rate for each year is shown in Figure 3. As expected from earlier research (*e.g.*, Hildner *et al.*, 1976; Howard *et al.*, 1985; St. Cyr *et al.*, 2000; Gopalswamy, 2006; Vourlidas *et al.*, 2010; Robbrecht, Berghmans, and van der Linden, 2009) the CME rate varies in phase with the sunspot number, a common historic indicator of solar activity, downloaded from the Solar Influences Data Analysis Center (http://sidc.oma.be). In the following section we will address the overlap of the endpoints of this period with the two space-based coronagraphs.

4. Mk3 CME Rate Compared to SMM C/P (1989) and SOHO LASCO (1996)

In order to consider the Mk3 CME rate in a historical context comparable to Webb and Howard (1994), we have "cross-calibrated" the end points of this period and taken advantage of the overlap with SMM C/P (1989) and with SOHO LASCO (1996). For those years we have examined each catalogued CME to determine which events were detected by both coronagraphs, and which events were missed by one of the two instruments. There are several reasons to expect the Mk3 detections of CMEs to be inferior to the space-based instruments: First, the Mk3 measured polarized brightness (pB), whereas C/P and LASCO measured total brightness (B). Observations in pB restrict detection of coronal features (and CMEs) to those that are closer to the plane of the sky than observations in B. This is a result of the Thomson scattering function of photospheric light by free electrons in the corona. An exhaustive quantification of this effect can be found in the appendix of Hundhausen (1993). Second, the scattered light background is expected to be higher for a ground-based instrument than a for an externally occulted space-based coronagraph. Third, the limited field of view and duty cycle of Mk3 compared to space-based instruments means CMEs will simply spend less time there. Fourth, any CMEs that originate higher in the corona than the Mk3 field of view may not have any signature in the low corona (*e.g.*, Kilpua *et al.*, 2014).

Paper1 reported several results concerning Mk3: a comparison of the statistical distributions of CMEs with SMM C/P and *Solwind*; a comparison of the properties of individual Mk3 events with SMM C/P; and the measurements of the initial acceleration of a large sample of CMEs. External factors have altered the Mk3 data archive since we examined the data

Table 2 Statistics from an event-by-event comparison during the overlap period of Mk3 with SMM C/P and SOHO LASCO.

	SMM C/P [1980 – 1989] from Paper1	SMM C/P [1989] this study	SOHO LASCO [1996] this study
CMEs detected by both	141	50	5
Spaceborne CMEs missed by Mk3	33	17	15
Fraction missed	33/174 = 19 %	17/67 = 25 %	15/20 = 75 %
Mk3 CMEs during spaceborne data gaps	95	16	1

for Paper1 – notably, a disk drive crash resulted in the necessity to completely rebuild the online dataset from a deep archive of raw data, so we elected to re-examine the 1989 dataset for the present study. We found that some data that had been available in 1999 were now lost, and in some cases new data had appeared. Additionally, a few new events were discovered (8 new events), and a number of events were lost or were downgraded from CMEs to "anomalies" (20 events). Paper1 was based on 78 CMEs in 1989; whereas the present study is based on 66 CMEs identified during that year.

Although the statistical distributions from the recent analysis appear almost identical to Paper1, we compared the measurements of the 58 events in common from the 1999 and this 2015 study. We found excellent agreement in the location measurements (average difference 2°), width measurements (average difference 3°), and speed measurements (average difference less than 100 $\mathrm{km\,s^{-1}}$).

In Table 2 we list the results of the comparison of SMM C/P CMEs with Mk3 from Paper1 (for completeness) and for the recent reexamination of the 1989 data. For both SMM C/P and SOHO LASCO, we examined all events where either the space-based CME start time or the extrapolated start time (if a speed was measured) was between 17:00 – 24:00 U.T., which is the nominal observing window for Mk3.

Webb and Howard (1994) reported a CME rate for 1989 of 2.0 events/day [duty-cycle corrected] based on the 10.5 months of SMM C/P observations. This was based on the Burkepile and St. Cyr (1993) tabulation of events and was duty-cycle corrected using the data gaps listed there. Although discussion continues about whether "stages" of eruption are actually separate CMEs (*e.g.*, Howard and DeForest, 2014), we now believe the SMM rate should be adjusted slightly higher due to undercounting "multiple part" events that were originally catalogued as single CMEs. When we make that adjustment (62 multiple-part events during 1989 results in an additional 82 CMEs), then we arrive at the 2.47 CMEs/day shown in Figure 3 and labeled SMM C/P. Nevertheless, the rate as determined by Mk3 is higher than the adjusted SMM value.

The 1996 – 1998 SOHO LASCO CMEs were described by St. Cyr *et al.* (2000). CME rates on both an annual and Carrington Rotation basis were tabulated, duty-cycle corrected, and we show that in Figure 3. Other researchers have examined the LASCO observations and reported different numbers of CMEs. Minor discrepancies in CME identification from the St. Cyr *et al.* (2000) paper were addressed in detail by Yashiro *et al.* (2004), who found that variations in counts were less than 7 %. Robbrecht, Berghmans, and van der Linden (2009) did not tally CMEs observed by LASCO during 1996, but the number of CME detections by their automated detection scheme (CACTus) were generally larger than reported by human

counts. Wang and Colaninno (2014) contend that it is the total ejected mass rather than number of CMEs that is correlated with the solar activity cycle.

The Mk3 CME rates in Table 1 and Figure 3 have been duty-cycle corrected, but they have not been adjusted for what Webb and Howard (1994) called "visibility function". As noted earlier, Thomson scattering is most efficient for CMEs and features near the solar limb (the plane of sky), and there is no method to directly characterize the overall detection sensitivity for a given coronagraph. Moreover, each coronagraph will have a background due to stray light below which coronal changes cannot be detected. The Webb and Howard (1994) visibility function was based on radio Type II bursts to correct for this inherent observing inefficiency for each instrument, thus yielding a global (360°) estimate for the CME rate.

As described in St. Cyr *et al.* (2000), the LASCO instruments were superior to previous coronagraphs for CME detection for a number of reasons. Two primary factors were that the CCD detectors provided a significant improvement in dynamic range; and the L-1 halo orbit provided a stable stray light background that was not previously achievable. In fact, Tripathi, Bothmer, and Cremades (2004) reported that 92% of EUV post-eruptive arcades (1997 – 2002) had associated LASCO CMEs, indicating that any visibility function correction for LASCO would be very small. The foundation for determining such a visibility function for Mk3, at least in a comparative sense, is contained in Table 2: the fraction of CMEs missed.

5. Discussion

We note that Table 1 shows that the annual number of observing days by Mk3 jumped markedly two times [1990 – 1991 and 1993 – 1994]. To explain this, we continue with the story of "synoptic-only" data and its impact on the CME rate estimation. For those millennial readers born post-1980, this explanation may be difficult to fathom, but in the pre-Internet, digital storage capacity-starved world that existed at the time these data were gathered, it makes complete sense. Through the 1980s and until 1991 the Mk3 images were transported on large format (1/2 inch, 9-track reel) computer tapes. Each tape could hold one hour's worth of data (20 images). The tapes had to be shipped from MLSO to HAO for processing, and then shipped back to Hawaii for re-use. The shipping costs to-and-from Mauna Loa to Boulder represented a significant fraction of the observatory's operating budget. To reduce financial stress, the "synoptic-only" program was instituted whereby only a few images were retained for that day if the observer-on-duty had not detected any CMEs. That program ended in 1989, and all data gathered from that point forward were retained.

The increase in annual observing time in early 1991 was a result of the transition from 1/2 inch reel tape to 8 mm compact tape, whereby an entire day's observation could fit easily on a single small tape, thus significantly reducing shipping costs. The second increase in annual observing time that is evident in 1994 was the result of hiring a third full-time observer to take advantage of those days where good seeing permitted extended observation.

What about the impact of the synoptic-only program on the CME rate estimation? Since some 1989 Mk3 data were discarded, we have had to use additional steps to determine both the duty cycle and the number of CMEs for that year. There were 68 days during 1989 where only synoptic data were retained, and we must assume that the data were examined and discarded because no CMEs were evident. It is important to note that the small observing team at MLSO was comprised of long-tenured professionals who worked with the instrument on a daily basis and were adept at recognizing small changes in the corona. There was a display on the observatory console that allowed them to monitor each individual image as it

was acquired. Although movies of direct and differenced images were not available, intensity contour plots (quantified to 6-levels) of the differences between any two Mk3 images could be displayed, so large-scale changes in the corona would have been detected. More importantly, a Hα chromospheric monitor was available for viewing the solar disk and limb in real-time, so the observers were aware of flares and prominence eruptions, noted such in the log, and retained the full Mk3 dataset during the synoptic-only years.

These facts explain why *any* very faint (brightness 1) CMEs were retained during the synoptic-only program years. Still, it is likely that some faint, and perhaps slow events were missed by the observers, so we must estimate how many events may have been unknowingly discarded. To obtain an estimate of the amount of discarded data in 1989, we have tallied the times of Mk3 operation from the hand-written observers' logs for those 68 synoptic-only days, and we found that 167 hours of observation were discarded. To calculate the CME rate for 1989 we have added this additional time to the observing time duration (scaled proportionally to reflect likely 10 minute gaps) to obtain a total equivalent observing time for the year. We have similarly scaled the number of images and that equivalent time in determining the duty cycle for 1989.

There were 66 CMEs recorded in 1989 during the 17.06 equivalent day's observation, and an additional 5.92 equivalent day's observation discarded [which is reflected in the 22.98 days in Table 1]. The best case for the discarded observations is that no CMEs were missed, so the 66 CMEs that we found represent the complete sample for that year. The worst case is that there were one-or-more very faint CMEs on each of the discarded 68 days, but that would yield a rate of more than 6 CMEs/day, which seems highly unlikely for the Mk3. Given the experience of the observers and the fact that the fraction of very faint CMEs during that year was comparable to other years (see Figure 2d), it seems most likely that only a few very faint events were discarded. The 163 observing days that were retained resulted in 66 CMEs, of which 21 were very faint. Assuming that a similar fraction of the 68 synoptic-only days had very faint events, then an additional 9 CMEs may have been discarded. Using those figures to estimate the uncertainties, we arrive at a conservative rate for that year of 3.1 ($+0.6$, -0.2) CMEs/day.

Why is the Mk3 CME rate for 1996 significantly less than that for LASCO? As described before, the superior sensitivity for LASCO is certainly a factor; but it seems likely that there is at least one additional cause. Since van de Hulst (1949) it has been known that the coronal brightness follows a solar cycle dependence. Fisher and Sime (1984) reported that the value of pB does not fall to zero at any point in the cycle based on Mk-coronameter measurements; however, there was a change of a factor of at least 2 in the amount of coronal mass between minimum and maximum phases. More recently, several researchers have noted that the average CME mass (and hence brightness) also varies in phase with the solar cycle (*e.g.*, MacQueen *et al.*, 2001; Vourlidas *et al.*, 2010). Recalling Paper1, there were very few CMEs detected in 1986, a year that was comparable to 1996 in terms of solar activity levels [average daily sunspot number: 13.4 (1986) versus 8.6 (1996); average 10 cm full-disk radio flux: 74.1 (1986) versus 71.9 (1996)]. Coincidentally, there were only six CMEs found in Mk3 data each of those years, and the coronal brightness level was at or near the threshold for detectability for Mk3. Thus it may be the case that the visibility function for Mk3 (and indeed, any coronagraph where stray light so dominates the desired signal) must be considered dependent on the solar cycle phase. This topic will be explored in a future manuscript using these data to complete the CME rate determination through the present time.

6. Conclusions

We have reported here a successful attempt to fill the 1990 – 1995 gap in the CME rate. We have used the Mauna Loa Solar Observatory's *Mark III* (Mk3) K-coronameter to identify and measure CMEs. We described the statistical properties of the CMEs detected during 1989 – 1996, and we determined an observing duty cycle, a CME rate, and an uncertainty in the rate for each of those years. We compared the Mk3-derived CME rate from 1989 with the rate from the SMM C/P coronagraph, and from 1996 with the rate from the SOHO LASCO coronagraphs. We also examined each event from the space-based coronagraphs to determine which events were also detected by Mk3. The derived Mk3 CME rates for 1989 through 1996 appear to track the solar activity cycle for those years.

Acknowledgements The Mauna Loa Solar Observatory is operated by the High Altitude Observatory, as part of the National Center for Atmospheric Research (NCAR). NCAR is supported by the National Science Foundation. The data were acquired through the hard work and dedication of the MLSO observers: K. Fisher, E. Yasukawa, C. Garcia, D. Chu, E. Lundin, P. Seagraves, and D. Koon. H. Xie was supported by NASA LWS grant number NNX15AB70G. The authors declare that they have no conflict of interest.

References

Biesecker, D.A., Lamy, P., St. Cyr, O.C., Llebaria, A., Howard, R.A.: 2002, Sungrazing comets discovered with the SOHO/LASCO coronagraphs 1996 – 1998. *Icarus* **157**, 323. DOI.

Brueckner, G.E., Howard, R.A., Koomen, M.J., Korendyke, C.M., Michels, D.J., Moses, J.D., *et al.*: 1995, The large angle spectroscopic coronagraph (LASCO). *Solar Phys.* **162**, 357.

Burkepile, J.T., St. Cyr, O.C.: 1993, A revised and expanded catalogue of coronal mass ejections observed by the Solar Maximum Mission coronagraph. In: *NCAR Tech Note TN-369+STR*, National Center for Atmospheric Research, Boulder.

De Wijn, A.G., Burkepile, J.T., Tomczyk, S., Nelson, P., Huang, P., Gallagher, D.: 2012, Stray light and polarimetry considerations for the COSMO K-coronagraph. *Proc. SPIE* **8444**, 84443N. DOI

Domingo, V., Fleck, B., Poland, A.I.: 1995, The SOHO mission: an overview. *Solar Phys.* **162**, 1.

Elmore, D.F., Burkepile, J.T., Darnell, J.A., Lecinski, A.R., Stanger, A.L.: 2003, Calibration of a ground-based solar coronal polarimeter. *Proc. SPIE* **4843**, 66.

Fisher, R., Sime, D.G.: 1984, Solar activity cycle variation of the K corona. *Astrophys. J.* **285**, 354.

Fisher, R.R., Lee, R.H., MacQueen, R.M., Poland, A.I.: 1981, New Mauna Loa coronagraph systems. *Appl. Opt.* **20**, 1094.

Garcia, C., Hansen, R., Hull, H., Lacey, L., Lee, R.: 1971, *Bull. Am. Astron. Soc.* **3Q**, 261.

Gopalswamy, N.: 2006, Consequences of coronal mass ejections in the heliosphere. *Sun Geosph.* **1**, 5.

Hansen, R.T., Garcia, C.J., Hansen, S.F.: 1969, Brightness variations of the white light corona during the years 1964 – 1967. *Solar Phys.* **7**, 417.

Hildner, E., Gosling, J.T., MacQueen, R.M., Munro, R.H., Poland, A.I., Ross, C.L.: 1976, Frequency of coronal transients and solar activity. *Solar Phys.* **48**, 127.

Howard, T.A., DeForest, C.E.: 2014, The formation and launch of a coronal mass ejection flux rope: a narrative based on observations. *Astrophys. J.* **796**, 33. DOI.

Howard, R.A., Sheeley, N.R. Jr., Koomen, M.J., Michels, D.J.: 1985, Coronal mass ejections 1979 – 1981. *J. Geophys. Res.* **90**, 8173.

Hundhausen, A.J.: 1993, Sizes and locations of coronal mass ejections: SMM observations from 1980 and 1984 – 1989. *J. Geophys. Res.* **98**, 13177.

Hundhausen, A.J., Burkepile, J.T., St. Cyr, O.C.: 1994, Speeds of coronal mass ejections: SMM observations from 1980 and 1984 – 1989. *J. Geophys. Res.* **99**, 6543. DOI.

Hundhausen, A.J., Stanger, A.L., Serbicki, S.A.: 1994, Mass and energy contents of coronal mass ejections: SMM results from 1980 and 1984 – 1988. In: *Proceedings of the Third SOHO Workshop*, *ESA* **SP-373**, 409.

Kilpua, E.K.J., Mierla, M., Zhukov, A.N., Rodriguez, L., Vourlidas, A., Wood, B.: 2014, Solar sources of interplanetary coronal mass ejections during the solar cycle 23/24 minimum. *Solar Phys.* **289**, 3773. DOI.

Lyot, B.: 1933, The study of the solar corona without an eclipse. *J. Roy. Astron. Soc. Can.* **27**, 265.

MacQueen, R.M., St. Cyr, O.C.: 1991, Sungrazing comets observed by the Solar Maximum Mission coronagraph. *Icarus* **90**, 96. DOI.

MacQueen, R.M., Csoeke-Poeckh, A., Hildner, E., House, L., Reynolds, R., Stanger, A., Tepoel, H., Wagner, W.: 1980, The High Altitude Observatory coronagraph/polarimeter on the Solar Maximum Mission. *Solar Phys.* **65**, 91.

MacQueen, R.M., Burkepile, J.T., Holzer, T.E., Stanger, A.L., Spence, K.E.: 2001, Solar coronal brightness changes and mass ejections during solar cycle 22. *Astrophys. J.* **549**, 1175.

Newkirk, G., Axtell, J., Wlerick, G.: 1957, Studies of the electron corona. *Astrophys. J.* **62**, 95.

Newkirk, G.A., Curtis, G.W., Watson, D.K., Manning, R., Shelby, J.: 1959, The inner solar corona during June 1959. *Nature* **184**, 1308.

Robbrecht, E., Berghmans, D., van der Linden, R.A.M.: 2009, Automated LASCO CME catalog for solar cycle 23: are CMEs scale invariant? *Astrophys. J.* **691**, 1222.

Shea, M.A., Cramp, J.L., Duldig, M.L., Smart, D.F., Humble, J.E., Fenton, A.G., Fenton, K.B.: 1995, Comparison of ground-level enhancements of 15 November 1960 and 22 October 1989. In: *Proc. ICRC* **4**, 208.

St. Cyr, O.C., Burkepile, J.T., Hundhausen, A.J., Lecinski, A.R.: 1999, A comparison of ground-based and spacecraft observations of coronal mass ejections from 1980 – 1989. *J. Geophys. Res.* **104**, 12493. DOI.

St. Cyr, O.C., Howard, R.A., Sheeley, N.R. Jr., Plunkett, S.P., Michels, D.J., Paswaters, S.E., Koomen, M.J., *et al.*: 2000, Properties of coronal mass ejections: SOHO LASCO observations from January 1996 to June 1998. *J. Geophys. Res.* **105**, 18169. DOI.

St. Cyr, O.C., Fleck, B., Davila, J.M.: 2014, The impact of coronagraphs. *Eos Trans. AGU* **95**, 369. DOI.

Tripathi, D., Bothmer, V., Cremades, H.: 2004, The basic characteristics of EUV post-eruptive arcades and their role as tracers of corona mass ejection source regions. *Astron. Astrophys.* **422**, 337. DOI.

van de Hulst, H.C.: 1949, Brightness variations of the solar corona. *Nature* **163**, 24.

Vourlidas, A., Howard, R.A., Esfandiari, E., Patsourakos, S., Yashiro, S., Michalek, G.: 2010, Comprehensive analysis of coronal mass ejection mass and energy properties over a full solar cycle. *J. Geophys. Res.* **722**, 1522. DOI.

Wang, Y.-M., Colaninno, R.: 2014, Is solar cycle 24 producing more coronal mass ejections than cycle 23? *Astrophys. J. Lett.* **784**, L27. DOI.

Webb, D.F., Howard, R.A.: 1994, The solar cycle variation of coronal mass ejections and the solar wind mass flux. *J. Geophys. Res.* **99**, 4201. DOI.

Wlerick, G., Axtell, J.: 1957, A new instrument for observing the electron corona. *Astrophys. J.* **126**, 253.

Woodgate, B.E., Maran, S.P.: 1986, The solar maximum mission repair – lessons learned. *Proc. SPIE* **729**, 202.

Yashiro, S., Gopalswamy, N., Michalek, G., St. Cyr, O.C., Plunkett, S.P., Rich, N.B., Howard, R.A.: 2004, A catalog of white light coronal mass ejections observed by the SOHO spacecraft. *J. Geophys. Res.* **109**, A07105. DOI.

Yashiro, S., Michalek, G., Gopalswamy, N.: 2008, A comparison of coronal mass ejections identified by manual and automatic methods. *Ann. Geophys.* **26**, 3103.